

See discussions, stats, and author profiles for this publication at: <https://www.researchgate.net/publication/44574205>

# Face-on Oriented Bilayer of Two Discotic Columnar Liquid Crystals for Organic Donor-Acceptor Heterojunction

ARTICLE *in* JOURNAL OF THE AMERICAN CHEMICAL SOCIETY · MAY 2010

Impact Factor: 12.11 · DOI: 10.1021/ja1012596 · Source: PubMed

---

CITATIONS

54

---

READS

31

3 AUTHORS, INCLUDING:



Eric Grelet

Centre de Recherche Paul Pascal

75 PUBLICATIONS 1,112 CITATIONS

SEE PROFILE

Face-on Oriented Bilayer of Two Discotic Columnar Liquid Crystals  
for Organic Donor–Acceptor Heterojunction

Olivier Thiebaut, Harald Bock, and Eric Grelet\*

Centre de Recherche Paul-Pascal, CNRS - Université de Bordeaux, 115 Avenue Schweitzer, 33600 Pessac, France

Received February 19, 2010; E-mail: grelet@crpp-bordeaux.cnrs.fr

Organic solar cells are based on a heterojunction resulting from the association of a donor and an acceptor material. Absorption of photons creates excitons which diffuse to the donor–acceptor interface, where they are dissociated into free charge carriers (holes and electrons respectively) by the local electric field. Donor–acceptor heterojunctions in organic photovoltaic devices can be created with two types of architectures, namely, bilayer (also called planar) heterojunctions and bulk heterojunctions.<sup>1a</sup> The main advantage of bulk heterojunction cells is to exhibit a wide donor–acceptor contact area, increasing the power conversion efficiency. However, such a geometry of interpenetrated networks is difficult to achieve and is not thermodynamically stable,<sup>1b</sup> suffering therefore from sensitivity toward aging. The lack of direct control of the bulk heterojunction morphology leads also in most cases to the formation of random-shaped domains within the photovoltaic device. An alternative approach to improve the conversion efficiency by the increase of both the exciton diffusion length and the charge carrier mobility is to significantly expand the structural order at large scales inside the heterojunction via the self-organization of two electronically complementary discotic compounds into liquid-crystalline phases.<sup>2</sup> Discotic columnar liquid crystals (CLCs) are known for their high exciton diffusion lengths and charge carrier mobilities along the columns when compared to conventional disordered materials used in organic solar cells.<sup>3</sup> Notably, the exciton diffusion length along the columns in typical triphenylene-based CLCs has been found to be of the order of 200 molecules, or 70 nm,<sup>4</sup> similar to the average thickness of an absorptive layer in an organic solar cell. In this work, we describe the realization of an *oriented bilayer heterojunction* by annealing-induced macroscopic self-assembly of two discotic materials. Our approach using ordered liquid-crystalline structures aims to eliminate the task to interdigitate the donor and acceptor domains by the stacking of two face-on (or homeotropically oriented) hexagonal columnar liquid crystals. This morphology is structurally favorable in terms of electronic properties and is invariant over time. Based on a pair of discotic CLCs which exhibit antagonist solubility and adjusted transition temperatures, we present here how homeotropic bilayers of such pairs of materials have been obtained by sequential thermal annealing of their codeposited mixtures.

Recently, a quite diverse family of materials exhibiting an appropriate hexagonal columnar liquid-crystalline phase at room temperature, namely arene-oligocarboxylic alkyl esters with racemic branched alkyl chains,<sup>5</sup> have been synthesized, and we have shown that homogeneous thin films of such materials can be obtained with the desired face-on alignment via a thermal annealing process through the liquid-to-CLC phase transition.<sup>6</sup> As a functional organic solar cell has to include not only one active layer of an appropriately oriented CLC but also both a columnar donor and a columnar acceptor layer in homeotropic orientation, we have set out to develop pairs of columnar materials which are essentially not miscible and whose alignment behavior can be managed. Despite a few approaches developed during the past few years, control of the phase separation between two discotic compounds remains challenging.<sup>7</sup> For instance, it has been shown that oligoethoxy-

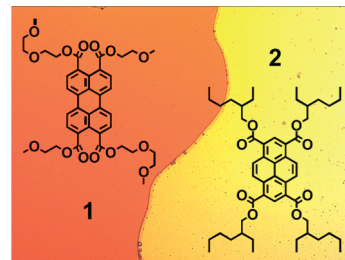


**Figure 1.** Schematic structure of the two compounds **1** (where only one of the two regioisomers is sketched) and **2**. Their low degree of miscibility is shown by a contact preparation between coverslip and glass slide in the isotropic liquid phase. Observation performed by bright field microscopy. The image size is 440  $\mu\text{m}$   $\times$  325  $\mu\text{m}$ .

ethylene side chains are able to render columnar liquid crystals soluble in polar solvents such as methanol or water and to induce microphase segregation within liquid-crystalline phases of materials that bear also apolar alkyl chains within the same molecules.<sup>8</sup> Although the water-soluble perylene-3,4,9,10-tetracarboxylic tetra-2-(2-(methoxy)ethoxy)-ethyl ester is not liquid-crystalline,<sup>9</sup> we found that the shorter chain ester **1** not only is soluble in methanol and insoluble in alkanes but also shows a hexagonal CLC phase at room temperature and up to a clearing transition to the isotropic liquid phase at approximately  $T_{\text{CLC1-Iso1}} = 148\text{ }^{\circ}\text{C}$  (see Supporting Information (SI)). We obtained **1** as a regioisomer mixture from perylene-3,4,9,10-tetracarboxylic dianhydride by 2-fold anhydride ring-opening with diethyleneglycol monomethylether followed by a 2-fold base catalyzed alkylation of the resulting diester-diacid with 2-bromoethyl methyl ether. Contact preparations of **1** with a room temperature hexagonal CLC material bearing conventional apolar alkyl chains such as pyrene-1,3,6,8-tetracarboxylic tetra-(2-ethyl)hexyl ester **2** ( $T_{\text{CLC2-Iso2}} = 91\text{ }^{\circ}\text{C}$ )<sup>5a</sup> shows that the two materials are almost immiscible even at an elevated temperature where both are in the isotropic liquid phase (Figure 1), as also confirmed by X-ray scattering and calorimetric studies (see SI). Moreover, **1** and **2** exhibit antagonist solubility, **2** being soluble in *n*-heptane, whereas **1** is completely insoluble. This specific solubility allows a *sequential* solution-processed deposition of the two discotic materials (on bare or ITO-covered glass slides or on silicon wafers with their oxide). After the successive deposition by spin-coating of **1** and **2** using chloroform and *n*-heptane respectively (see SI), each layer of a few hundred nanometers thick exhibits a degenerate planar alignment.<sup>6</sup> The bilayer is then heated up to  $\sim 150\text{ }^{\circ}\text{C}$ , where **1** and **2** are in the isotropic liquid phase (Iso1 and Iso2, respectively, in Figure 2a), before being cooled down at  $5\text{ }^{\circ}\text{C}/\text{min}$ . At  $\sim 135\text{ }^{\circ}\text{C}$ , dendritic domains of **1** in the homeotropic orientation appear (CLC1 in Figure 2b), whereas the upper layer of **2** is still in the isotropic liquid phase. Note that the decrease of  $T_{\text{CLC1-Iso1}}$  of a few degrees can be attributed to some supercooling at this cooling rate and also to the tiny amount of **2** mixed with **1** (see SI). At  $89\text{ }^{\circ}\text{C}$ , the second columnar mesophase (CLC2 in Figure 2d) nucleates on the top of the CLC1 layer. The hexagonal germ of CLC2 characteristic of a face-on orientation expands

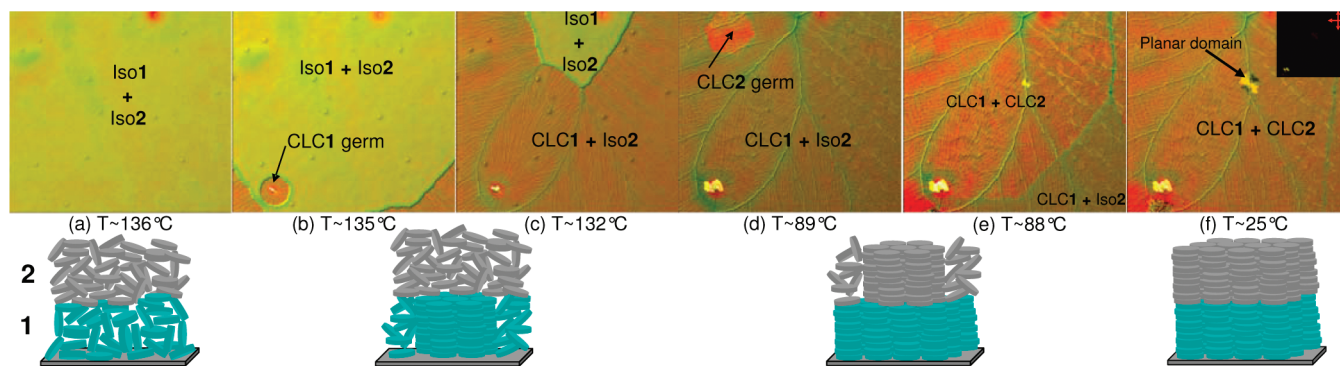


**Figure 2.** Growth by thermal annealing of a homeotropically oriented open bilayer (cooling rate: 5 °C/min) observed by differential interference contrast microscopy. In a preliminary step, both compounds **1** and **2** have been sequentially deposited by spin-coating before (a) being heated up to their isotropic liquid phase (Iso1 and Iso2, respectively). (b, c) Nucleation of the compound **1** in the columnar liquid-crystalline phase (CLC1) with a dendritic texture, while the upper layer (compound **2**) is still in its isotropic liquid phase (Iso2). (d, e) Growth of CLC2 above CLC1. Note the apex angle of the CLC2 growing domain of  $\sim 120^\circ$  characteristic of a face-on alignment. (f) Both layers exhibit a homeotropic alignment, as confirmed in the inset by the lack of birefringence between crossed polarizers. The layer thicknesses are approximately 350 and 200 nm for compounds **1** and **2**, respectively. The image size is  $715 \mu\text{m} \times 650 \mu\text{m}$ .

over all the sample area (Figure 2e). This demonstrates good wetting of the upper layer of CLC2 on CLC1 and leads to the following relation between the anisotropic surface tensions associated with the homeotropic anchoring,  $\gamma^\perp$ :

$$\gamma_{\text{CLC1-air}}^\perp > \gamma_{\text{CLC1-CLC2}}^\perp + \gamma_{\text{CLC2-air}}^\perp \quad (1)$$

This shows the stabilizing role of the upper discotic layer of **2** for managing a continuous face-on aligned CLC1 film. Moreover, the realization of the inverse heterojunction (with CLC2 as first layer and CLC1 as top layer) leads to strong dewetting with the formation of droplets. The existence of a few small birefringent side-on domains evidenced by polarizing microscopy (inset of Figure 2f) emphasizes the lack of optical anisotropy associated with the face-on orientation of each layer in the heterojunction. The homeotropic alignment of the bilayer is confirmed by transmission X-ray diffraction, with the presence of two X-ray patterns exhibiting a 6-fold symmetry (Figure 3), which are the signature of the homeotropic orientation of each layer. To increase X-ray transmission, very thin glass (80  $\mu\text{m}$  thick, Corning Inc.) has been used as a solid substrate. The more intense signal at smaller wavevector  $q = 3.5 \text{ nm}^{-1}$  corresponds to CLC2. The lower intensity at larger  $q = 4.1 \text{ nm}^{-1}$  associated with CLC1 stems from partial absorption of the scattered X-ray signal by the upper layer **2** of the heterojunction. Note that no epitaxial relations leading to a correlated orientation between the two compounds within the plane of the sample have to be inferred from Figure 3 (see SI).

In summary, the present work reports the achievement of a face-on oriented bilayer heterojunction formed by a pair of discotic materials designed with specific properties: selective solubility, low degree of miscibility, adjusted transition temperatures, and room temperature hexagonal columnar liquid-crystalline phase. The

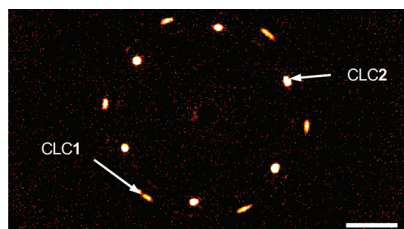


**Figure 3.** X-ray diffraction pattern of the homeotropically oriented bilayer in the geometry of an open supported thin film. The two 6-fold symmetries are the signature of the face-on (homeotropic) alignment of the two hexagonal columnar mesophases. Experiment performed in transmission with the X-ray beam normal to the plane of the substrate. The scale bar indicates  $2 \text{ nm}^{-1}$ .

homeotropic orientation of the open bilayer formed by these two compounds of only a few hundred nanometers thick has been demonstrated by both optical microscopy and X-ray scattering. This represents the first proof of principle of an organic heterojunction based on two oriented columnar liquid crystal layers.

**Acknowledgment.** This research is supported by ANR grants.

**Supporting Information Available:** Synthesis of **1**, physical characterizations of **1** and **2** and of their blend (X-ray diffraction and differential scanning calorimetry), film preparation, calibration of layer thicknesses, and optical absorption of the aligned heterojunction. This material is available free of charge via the Internet at <http://pubs.acs.org>.

## References

- (a) Heremans, P.; Cheyns, D.; Rand, B. P. *Acc. Chem. Res.* **2009**, *42*, 1740–1747. (b) Roncali, J. *Acc. Chem. Res.* **2009**, *42*, 1719–1730.
- Pisula, W.; Zorn, M.; Chang, J. Y.; Müllen, K.; Zentel, R. *Macromol. Rapid Commun.* **2009**, *30*, 1179–1202.
- (a) Laschat, S.; Baro, A.; Steinke, N.; Giesselmann, F.; Hägele, C.; Scalia, G.; Judele, R.; Kapatsina, E.; Sauer, S.; Schreivogel, A.; Tosoni, M. *Angew. Chem., Int. Ed.* **2007**, *46*, 4832–4887. (b) Sergeyev, S.; Pisula, W.; Geerts, Y. H. *Chem. Soc. Rev.* **2007**, *36*, 1902–1929. (c) Pouzet, E.; De Cupere, V.; Heintz, C.; Andreasen, J. W.; Breiby, D. W.; Nielsen, M. M.; Viville, P.; Lazzaroni, R.; Gbabode, G.; Geerts, Y. H. *J. Phys. Chem. C* **2009**, *113*, 14398–14406.
- Markovitsi, D.; Marguet, S.; Bondkowski, J.; Kumar, S. *J. Phys. Chem. B* **2001**, *105*, 1299–1306.
- (a) Hassheider, T.; Benning, S. A.; Kitzerow, H. S.; Achard, M. F.; Bock, H. *Angew. Chem., Int. Ed.* **2001**, *40*, 2060–2063. (b) Saïdi-Besbes, S.; Grelet, E.; Bock, H. *Angew. Chem., Int. Ed.* **2006**, *45*, 1783–1786. (c) Bock, H.; Rajaoarivelo, M.; Clavaguera, S.; Grelet, E. *Eur. J. Org. Chem.* **2006**, 2889–2893.
- (a) Grelet, E.; Bock, H. *Europhys. Lett.* **2006**, *73*, 712–718. (b) Charlet, E.; Grelet, E. *Phys. Rev. E* **2008**, *78*, 041707. (c) Charlet, E.; Grelet, E.; Brettes, P.; Bock, H.; Saadaoui, H.; Cisse, L.; Destruel, P.; Gherardi, N.; Seguy, I. *Appl. Phys. Lett.* **2008**, *92*, 024107. (d) Cisse, L.; Destruel, P.; Archambeau, S.; Seguy, I.; Jolinat, P.; Bock, H.; Grelet, E. *Chem. Phys. Lett.* **2009**, *476*, 89–91.
- (a) Wu, J.; Pisula, W.; Müllen, K. *Chem. Rev.* **2007**, *107*, 718–747, and references therein. (b) Zucchi, G.; Viville, P.; Donnio, B.; Vlad, A.; Melinte, S.; Mondeshki, M.; Graf, R.; Spiess, H. W.; Geerts, Y. H.; Lazzaroni, R. *J. Phys. Chem. B* **2009**, *113*, 5448–5457. (c) De Luca, G.; Liscio, A.; Melucci, M.; Schnitzler, T.; Pisula, W.; Clark, C. G.; Scolaro, L. M.; Palermo, W.; Müllen, K.; Samori, P. *J. Mater. Chem.* **2010**, *20*, 71–82. (d) Schweicher, G.; Gbabode, G.; Quist, F.; Debever, O.; Dumont, N.; Sergeyev, S.; Geerts, Y. H. *Chem. Mater.* **2009**, *21*, 5867–5874.
- (a) Boden, N.; Bushby, R. J.; Lu, Z.; Lozman, O. R. *Liq. Cryst.* **2001**, *28*, 657–661. (b) Lee, M.; Kim, J.-W.; Peleshanko, S.; Larson, K.; Yoo, Y.-S.; Vaknin, D.; Markutsya, S.; Tsukruk, V. V. *J. Am. Chem. Soc.* **2002**, *124*, 9121–9128. (c) Sakurai, T.; Shi, K.; Sato, H.; Tashiro, K.; Osuka, A.; Saeki, A.; Seki, S.; Tagawa, S.; Sasaki, S.; Masunaga, H.; Osaka, K.; Takata, M.; Aida, T. *J. Am. Chem. Soc.* **2008**, *130*, 13812–13813. (d) Feng, X.; Pisula, W.; Kudernac, T.; Wu, D.; Zhi, L.; De Feyter, S.; Müllen, K. *J. Am. Chem. Soc.* **2009**, *131*, 4439–4448. (e) Wicklein, A.; Lang, A.; Muth, M.; Thelakktat, M. *J. Am. Chem. Soc.* **2009**, *131*, 14442–14453.
- Arnaud, A.; Belleney, J.; Boué, F.; Bouteiller, L.; Carrot, G.; Wintgens, V. *Angew. Chem., Int. Ed.* **2004**, *43*, 1718–1721.

JA1012596

# Supporting Information

## Face-on oriented bilayer of two discotic columnar liquid crystals for organic donor-acceptor heterojunction

Olivier Thiebaut, Harald Bock, and Eric Grelet\*

Centre de Recherche Paul Pascal, CNRS - Université de Bordeaux

115 Avenue Schweitzer, 33600 Pessac, France

E-mail: grelet@crpp-bordeaux.cnrs.fr

### 1. Synthesis of compound 1 (*3,9(10)-bis(2-methoxyethoxycarbonyl)-4,10(9)-bis(2-(2-methoxyethoxy)ethoxycarbonyl)perylene*)

PTCDA (10g, 25.5mmol) is stirred with potassium carbonate (10g, 72mmol), 2-(2-methoxyethoxy)ethanol (50g, 0.4mol) and 2-methoxyethyl bromide (30g, 0.2mol) at 70°C for 24h. Ethyl acetate (1L) is added, the solids are filtered off, and solvent and methoxyethyl bromide are evaporated under vacuum. The resulting liquid is dissolved in chloroform (1L), and this solution is shaken with water (500ml); the resulting emulsion is phase separated by passing through a large glass filter, the water phase is discarded, and the chloroform is evaporated. The resulting viscous liquid, which sticks to the flask wall, is washed three times with water (100ml), and purified by column chromatography (silica gel, dichloromethane:acetone, first 5:1 to elute impurities, then 3:1 to elute product). Yield: 6.3g (8.4mmol, 33%).

<sup>1</sup>H NMR (400 MHz, CDCl<sub>3</sub>):  $\delta$  = 8.13 (d,  $J=8\text{Hz}$ , 4H, ArH), 7.99 (d,  $J=8\text{Hz}$ , 2H, ArH), 7.98 (d,  $J=8\text{Hz}$ , 2H, ArH), 4.53-4.47 (m, 8H, CO<sub>2</sub>CH<sub>2</sub>), 3.91-3.87 (m, 4H, OCH<sub>2</sub>), 3.79-3.75 (m, 4H, OCH<sub>2</sub>), 3.73-3.69 (m, 4H, OCH<sub>2</sub>), 3.58-3.54 (m, 4H, OCH<sub>2</sub>), 3.44 (s, 6H, OCH<sub>3</sub>), 3.36 (s, 6H, OCH<sub>3</sub>) ppm.

<sup>13</sup>C NMR (100 MHz, APT, CDCl<sub>3</sub>):  $\delta$  = 168.4 (2×CO<sub>2</sub>), 168.35 (2×CO<sub>2</sub>), 133.0 (4×C<sub>Ar</sub>), 130.7 (4×C<sub>Ar</sub>H), 129.8 (4×C<sub>Ar</sub>), 128.9 (2×C<sub>Ar</sub>), 128.6 (2×C<sub>Ar</sub>), 121.4 (4×C<sub>Ar</sub>H), 71.9 (2×CH<sub>2</sub>), 70.6 (2×CH<sub>2</sub>), 70.3 (2×CH<sub>2</sub>), 69.0 (2×CH<sub>2</sub>), 64.5 (2×CH<sub>2</sub>), 64.4 (2×CH<sub>2</sub>), 59.1 (2×CH<sub>3</sub>), 59.0 (2×CH<sub>3</sub>) ppm.

### 2. Physical characterizations of the discotic compounds 1 and 2

#### 2.1. Powder X-ray diffractograms

The two compounds, **1** and **2**, were placed in a glass capillary tube of diameter 1.5mm, and probed by a rotating anode X-ray generator (Rigaku) with a wavelength of 1.54Å and a sample-to-detector distance

of 133mm. The columnar mesophase exhibited by both discotic materials is of hexagonal symmetry, as shown in Figure S1 by X-ray diffraction.

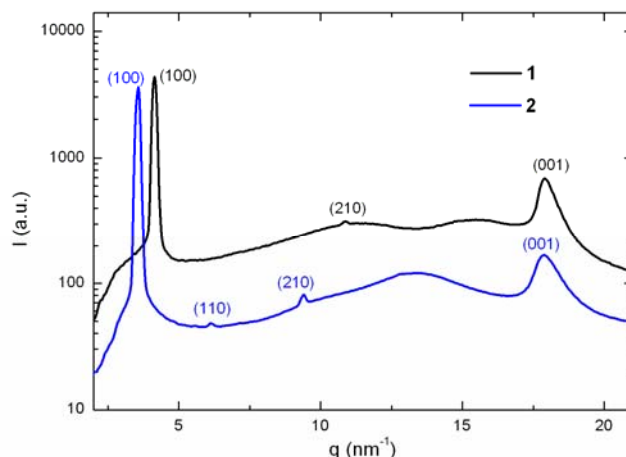


Figure S1. Powder X-ray diffractogram at room temperature of the two discotic compounds CLC1 (black line) and CLC2 (blue line), showing the Bragg reflections as the typical signature of a hexagonal packing of columns<sup>1</sup>. The (001) broad peak is characteristic of the liquid-like  $\pi$ -stacking of the discotic molecules within the columns.

## 2.2. Differential scanning calorimetry (DSC)

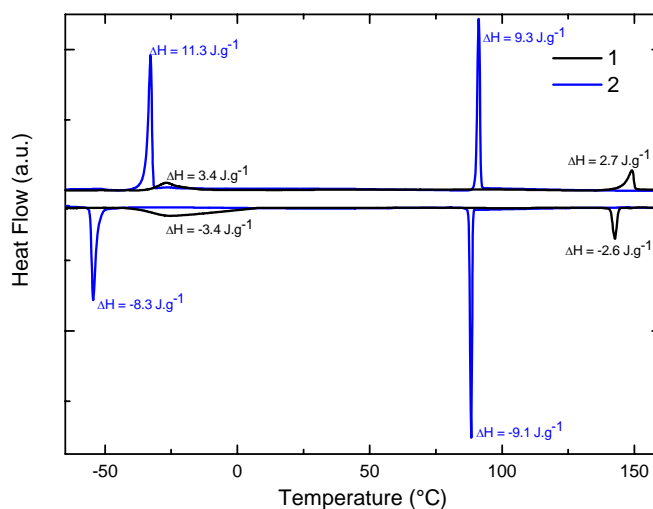


Figure S2. DSC thermograms of the two discotic compounds **1** (black line) and **2** (blue line) on heating and on cooling at 3°C/min.

Both materials, **1** and **2**, were studied by differential scanning calorimetry (Perkin Elmer), which reveal two phase transitions on each compound. For **1**, the first transition occurring on heating at -27°C is characteristic of a glass transition, as shown by its broad peak (Figure S2), whereas the second transition at 148°C accounts for the columnar liquid crystal to isotropic liquid phase transition. The thermogram

associated with **2** exhibits first the fusion at  $-33^{\circ}\text{C}$  (and reversibly a crystallization with a pronounced supercooling at  $-54^{\circ}\text{C}$ ) to a columnar mesophase, which melts into its isotropic liquid phase at  $91^{\circ}\text{C}$ .

### 3. Physical characterizations of the blend (1+2)

Several blends composed of different mass fractions of the two discotic compounds **1** and **2** were prepared in solution using chloroform as solvent. The latter was removed by evaporation at a temperature of  $130^{\circ}\text{C}$ . In order to show the low miscibility of the two discotic compounds **1** and **2**, both DSC and X-ray diffraction experiments were performed on bulk samples.

#### 3.1. Differential scanning calorimetry

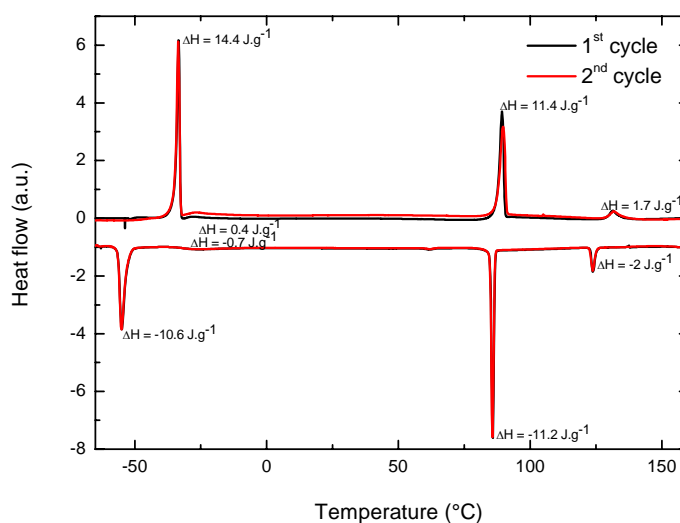


Figure S3. DSC thermograms of the blend composed of 50 wt % of **1** in **2** on heating and on cooling at  $3^{\circ}\text{C}/\text{min}$ . The first cycle is represented with a black line, and the second cycle with a red line.

Calorimetric studies were done with blends of different compositions. An example is given in Figure S3 with a blend formed by 50 wt % of **1** in **2**. The main result is that such thermogram is very similar to the superposition of thermograms of both compounds independently measured (Figure S2). Four peaks exist, with roughly the same enthalpies and only a small shift in temperature, showing that the blend exhibits identical phase transitions with respect to both compounds independently probed. On heating, the first transition corresponds to the fusion from crystal **2** into CLC2 at  $-33^{\circ}\text{C}$ , and the second one to the glass transition of **1** at  $-27^{\circ}\text{C}$ . The melting of CLC2 into Iso2 occurs at  $89.5^{\circ}\text{C}$ , followed by the fusion of CLC1 into its isotropic liquid phase, Iso1, at  $132^{\circ}\text{C}$ . Note that the characteristics of the blend remain unchanged after a second thermal cycle (Figure S3). Similar measurements were performed on blends with different compositions and the results are reported in Figure S4. In details, these investigations



indicate that only a tiny fraction of **2** (of about 2 wt %) can be incorporated in **1**, the transition temperature of the blend being constant (of about 132°C) for higher mass fractions. Conversely, only a small amount (around 5 wt %) of **1** can be homogeneously mixed with **2**. Note that below 8 wt % of **2** in **1**, the phase transition associated with **2** is difficult to record due to the low mass involved in the experiment.

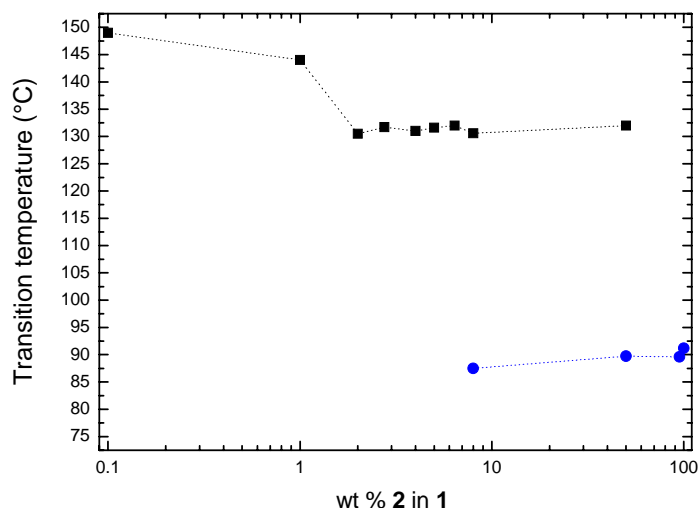


Figure S4. Temperature obtained by DSC of the phase transition from the columnar liquid crystal to the isotropic liquid phase for different blends mainly formed by **1** (black squares) and **2** (blue dots).

In summary, the calorimetric studies demonstrate that the two compounds **1** and **2** are essentially non-miscible, both in the hexagonal columnar mesophase and in the isotropic liquid phase. Indeed, no more than a few wt % of each compound in the other one can be homogeneously mixed.

### 3.2. Powder X-ray diffractograms

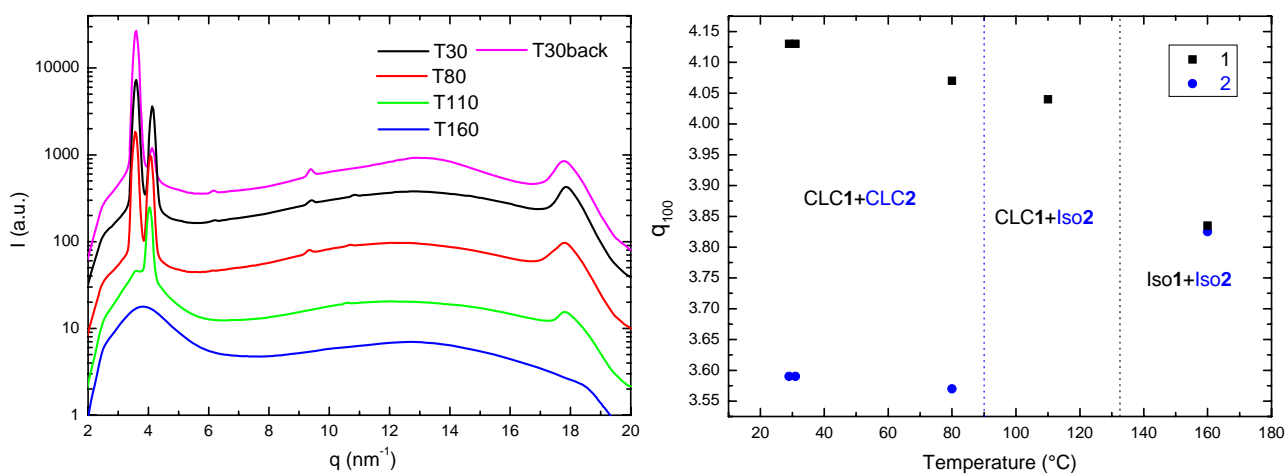


Figure S5. Left: Temperature dependence (black line: 30°C, red line: 80°C, green line: 110°C, blue line: 160°C, pink line: back to 30°C) of powder X-ray diffractograms of a blend composed of 50 wt % of **1** in **2**. Right: Evolution with temperature of the position of the first order Bragg reflection (100).

To confirm the low degree of miscibility of both compounds **1** and **2**, X-ray diffraction measurements were carried out on a blend formed by 50 wt % of **1** in **2**. The sample was prepared in a glass capillary tube (diameter 1.5mm), which was placed in a home-made heating stage transparent to X-ray wavelengths. The exposure time for each temperature was 4 hours. Two sharp Bragg peaks at 3.6 and 4.1nm<sup>-1</sup> account for the intercolumnar ordering, at room temperature, of CLC2 and CLC1 respectively (Figure S5). At 80°C, dilatation of both hexagonal lattices leads to smaller values of the corresponding Bragg reflections. The melting of each compound into its isotropic liquid phase is revealed by both the broad peak characteristic of short ranged positional order, and by the suppression at higher q (around 18nm<sup>-1</sup>) of the peak associated with the  $\pi$ -stacking of the discotic molecules (Figure S5). After a few hours at high temperature (160°C), the sample is cooled down to ambient temperature where the initial values of each hexagonal lattice are recovered (Figure S5), confirming that the very low miscibility of the compounds does not induce a change of each hexagonal lattice parameter.

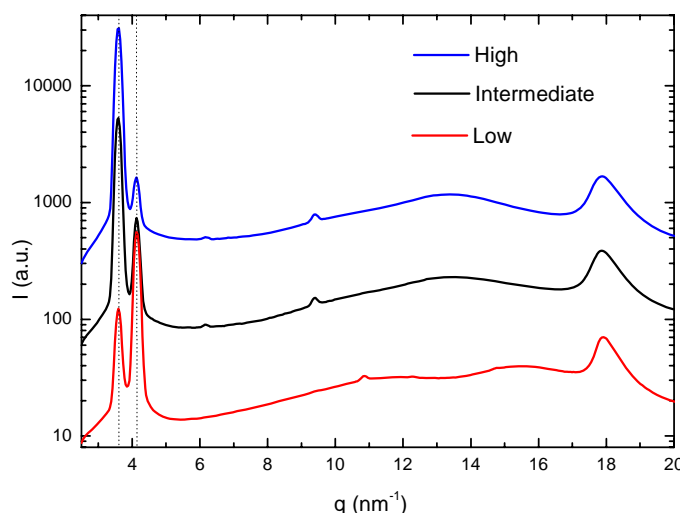


Figure S6. Scattered intensity at room temperature of a blend composed of 50 wt % of **1** in **2** after thermal annealing recorded at different positions in the capillary tube. The variation of intensity along the height of the sample shows the concentration gradient issued from the macroscopic phase separation occurring between the two materials.

More precisely, if the positions of the Bragg reflections are unchanged after thermal annealing, their intensity has varied as a consequence of the macroscopic phase separation occurring at high temperature. Indeed, the density of compound **1** is higher than **2**, leading to a progressive demixing in the fluid isotropic liquid phases. This has been evidenced by probing by X-ray diffraction different positions in the capillary tube, where the intensity of the Bragg peak (around 3.6nm<sup>-1</sup>) associated with CLC2 is the



highest on the top. Conversely, the intensity of Bragg reflection corresponding to CLC1 (around  $4.1\text{nm}^{-1}$ ) is maximal on the bottom. Thus no specific interaction between the two materials has been evidenced.

## 4. Film preparation, optical characterizations and bilayer X-ray scattering

### 4.1. Substrate surface treatment and film deposition

Two solid substrates have been used, thin glass slides (Corning Inc.) and silicon wafers with their oxide (Siltronix) for X-ray diffraction and optical microscopy experiments, respectively. They were first cleaned following a standard procedure<sup>2</sup> with three successive ultrasound baths of distilled water, acetone and ethanol. They were then dipped into sulfochromic acid before being rinsed with distilled water, and dried with nitrogen. The substrates were then coated with discotic materials by spin-coating. A liquid crystal solution of a few wt % in a specific solvent (chloroform and n-heptane for **1** and **2**, respectively) is spin-coated at 2000 rpm during 30 seconds on the previously cleaned substrates. The film thicknesses were measured by using an atomic force microscope in tapping mode acting as a mechanical profilometer. The result of the calibration of the film thickness vs. concentration is given in Figure S3.

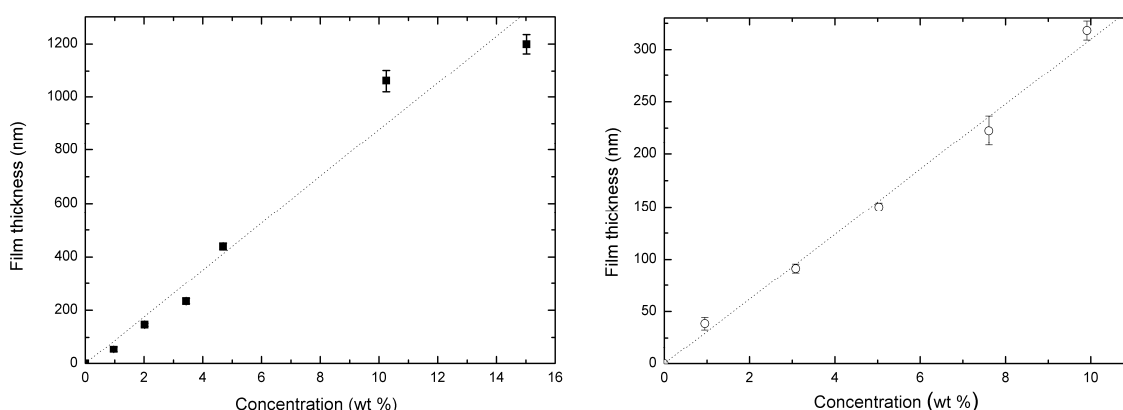


Figure S7. Film thickness as a function of the compound concentration during spin-coating deposition for **1** in chloroform (full squares) and **2** in n-heptane (open circles). The dotted line represents in each case a linear fit.

### 4.2. Optical measurements

Optical observations were done with an optical microscope (Olympus, BX51), combined with both a color CCD camera (JAI, CV-M7) and a heating stage (Mettler FP90). Two contrast modes were used to study the orientation of the columnar liquid crystal films, either between crossed polarizers or by differential interference contrast (DIC). The DIC technique is sensitive to the refractive index gradient, and therefore improves the contrast of optically isotropic samples by enhancing all interfaces such as grain boundaries between liquid crystalline domains and dendrites.

### 4.3. Bilayer light absorption

In order to provide another confirmation of the face-on organization of both layers in the heterojunction, the absorption spectrum of an aligned heterojunction and of each compound in homeotropic orientation has been independently measured. The experimental validation is based on the fact that the face-on alignment corresponds, for discotic compounds, to the orientation of maximal absorption<sup>2</sup> (The absorption intensity in planar orientation at same thickness being about two times smaller). Absorption spectra were obtained by using a spectrophotometer (Unicam UV-Vis spectrometer, UV4-500), and were recorded with a scan speed of 120 nm/min. Two films of **1** and **2** on two glass substrates were initially deposited by spin-coating with a concentration of 6.2 wt% in chloroform and 9.8%wt in n-heptane, respectively. According to Figure S3, the corresponding film thickness is 540nm and 300nm for the compounds **1** and **2** respectively. The resulting absorption of each compound is given in Figure S4, as well as the arithmetic sum of the two spectra (black dashed line). This sum of the two spectra is in very good agreement with the absorption of a face-on aligned heterojunction made of two layers of **1** and **2** having an identical thickness (red line in Figure S4). This result confirms the homeotropic alignment of each layer in the heterojunction.

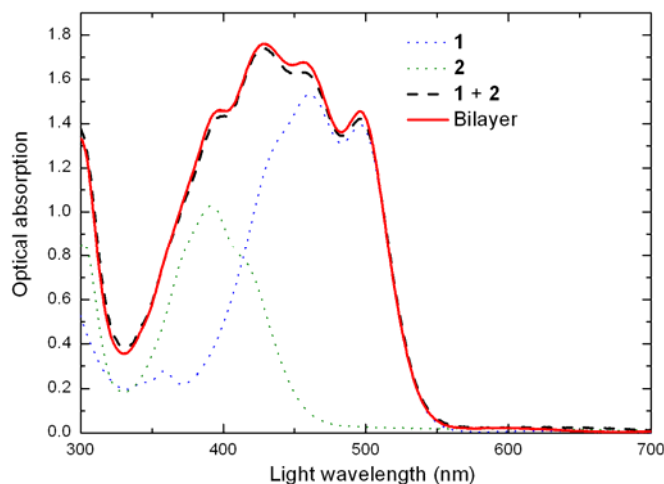


Figure S8. Absorption spectra of homeotropically aligned columnar liquid crystal films of the compounds **1** and **2** (blue and green dotted lines, respectively), of the arithmetic sum of **1** and **2** (black dashed line), and of the bilayer of **1** and **2** (red line) having an identical thickness.

### 4.4. Bilayer X-ray diffraction

The average radial intensity profile of the X-ray diffractogram (Figure 3) of the homeotropically oriented bilayer is shown in Figure S9. The position of the first order Bragg peak associated with each compound is similar to the values obtained in bulk (Figure S1). Note that the lower intensity at larger  $q$  for CLC**1**

stems from partial absorption of the scattered X-ray signal by the upper layer **2** of the heterojunction.

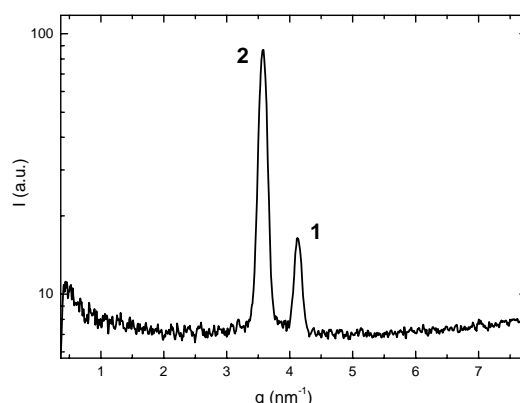


Figure S9. Scattered intensity as a function of the wave vector  $q$  corresponding to the X-ray diffractogram associated with the homeotropically oriented bilayer shown in Figure 3. The two peaks correspond to first Bragg reflection (100) of the two hexagonal columnar liquid crystalline phases, CLC2 and CLC1 respectively.

To demonstrate that no epitaxial relations exist between the two homeotropically oriented CLC layers of the Figure 3, we present in Figure S10 two other X-ray diffraction patterns, which show that a single domain of each compound can coexist with domains of the other compound exhibiting simultaneously different orientations.

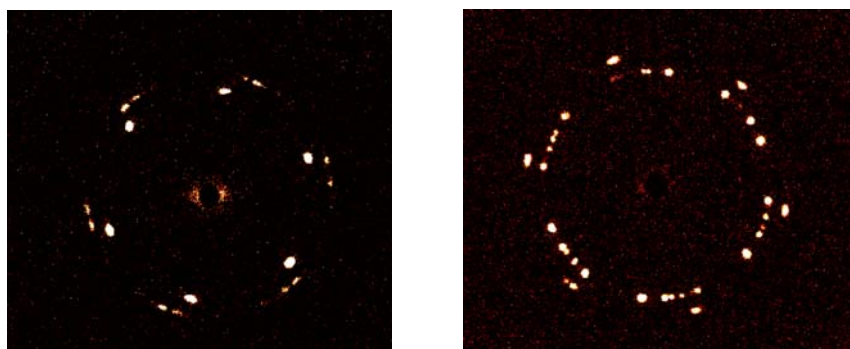


Figure S10. X-ray diffraction pattern of homeotropically oriented bilayers in the geometry of open supported thin film (Same conditions as in Figure 3). Left: Single hexagonal domain of CLC2 in coexistence with two domains of CLC1. Right: Single domain of CLC1 in coexistence with five hexagonal domains of CLC2.

## References

- (1) Laschat, S.; Baro, A.; Steinke, N.; Giesselmann, F.; Hägele, C.; Scalia, G.; Judele, R.; Kapatsina, E.; Sauer, S.; Schreivogel, A.; Tosoni, M. , *Angew. Chem. Int. Ed.* **2007**, *46*, 4832-4887.
- (2) Charlet, E.; Grelet, E. *Phys. Rev. E* **2008**, *78*, 041707.